Supporting Information

Linking Renewable Cellulose Nanocrystal into Lightweightand highly elastic Carbon Aerogel

Hao Zhuo, Yijie Hu, Zehong Chen, Xinwen Peng, Haihong Lai, Linxiang Liu, Qingzhong Liu, Chuanfu Liu, and Linxin Zhong*

State Key Laboratory of Pulp and Paper Engineering, South China University of Technology, Guangzhou, 510641, China.

*E-mail: lxzhong0611@scut.edu.cn (L. Zhong)

Number of pages: 27
Number of tables: 3
Number of figures: 11

Experiment section

Preparation of CNC. 15.0 g cellulose was added into 150 mL 64 wt% H_2SO_4 solution, and the mixture was stirred at 55 °C for 60 min. Then the reaction was stopped by adding 1 L cold deionized water, and the suspension was centrifuged for 10 min (5000 rpm) for 2 times to separate the CNC. The obtained CNC was dialyzed against deionized water for 2 days to obtain CNC suspension with 2.5 wt% concentration.

Fabrication of carbon aerogels. Firstly, 6.4 g CNC suspension (2.5 wt%, 160 mg CNC) and 160 mg KGM powder were dispersed in 33.6 g deionized water, stirred for 10 min, and then ultrasonicated for 30 min to make sure that KGM were sufficiently dissolved and CNC dispersed. After that, 13 mL of above mixture was placed in a plastic box (38 mm × 29 mm ×18 mm) and tied to an open lidless steel box. Then, liquid nitrogen was added into the steel box to create a temperature gradient, whereas parallel ice columns with long-range alignment formed because of the growth of ice nucleus along horizontal direction. The samples were freeze-dried to obtain KGM/CNC aerogel. The samples were freeze-dried to obtain KGM/CNC aerogels (the volume was about 13 cm^3). For comparison, pure KGM (8 mg/mL) and, CNC (8 mg/mL) aerogels and KGM/CNC aerogel with different ratios and concentrations were also prepared with the same process. Specifically, samples with different mass ratios of CNC to KGM (1:3, 1:2, 1:1, and 1:2 respectively) were also fabricated (total concentration is 0.8%). Samples with different concentrations were prepared at a ratio of 1:1 (CNC: KGM). The aerogels were carbonized in a tube furnace via a two-stage

process under N_2 atmosphere. The first stage was carried out from 30 °C to 200 °C with a heating rate of 5 °C min^{-1} and held for 2 h. In the second stage, sample was pyrolyzed from 200 °C to 700 °C with a heating rate of 3 °C min^{-1} and then held for another 2 h to obtain carbon aerogels C-KGM, C-KC and C-CNC.

Compression, elasticity, fatigue resistance and compression-responding conductivity. Compression, elasticity and cycling tests were performed on an Instron 5565 equipped with a 50 N load cell. Cuboidal sample (about 25 mm × 20 mm × 11 mm) was placed between two compression stages with the top stage applying uniaxial compression and release on carbon aerogel along the vertical direction. The resistance of carbon aerogel was recorded using a multimeter (VC 890D), and the electrical current was recorded on an electrochemical workstation (CHI660E).

Assembly and sensing test of compressible and wearable sensor. The sensor was fabricated by placing the biomass-derived aerogel (the thickness of aerogel was controlled at 1 mm by cutting) between two Ni electrodes adhered to 10-μm-thick poly (ethylene terephthalate) (PET) substrates. The real-time current signals were recorded on a 2400 digital source-Meter and CHI660E electrochemical workstation (Shanghai Chenhua Instruments Corp., Shanghai, China Co).

Real-time current signal of wearable sensor. A plain and arc-shaped PET (150-μm-thick) sheet with Ni electrode were used to sandwich the as-prepared aerogel,

and the distances between PET sheets were about 1 mm for bending test. The real-time current signals were recorded on a 2400 digital source-Meter.

Characterizations. Raman spectra were recorded on a Raman spectrometer (LabRAM ARAMIS-Horiba JobinYvon) operating with 532 nm laser. XRD patterns were measured on a Bruker D8 diffractometer. Micromorphology was characterized with TEM (JEM-2100F) and SEM (Merlin, Zeiss). X-ray photoelectron spectra (XPS) were recorded on Thermo Scientific Thermo SCIENTIFIC K-ALPHA with an exciting source of Al•Kα (1286.6 eV). TGA-FTIR of aerogels was performed on a simultaneous thermal analyzer (NETZSCH STA 449F5). The porosity was tesed on AutoPore IV 9500 (Micromeritics Instrument Corporation). A total of 5.0–10.0 mg of sample was placed in an aluminum pan, and heated from ambient temperature to 200 °C at a heating rate of 15 °C min^{-1}, and then heated to 700 °C at a heating rate of 3 °C min^{-1} in a nitrogen atmosphere with a flush rate of 25 mL min^{-1}.

Finite Element Simulations. The large geometric deformation and elastic behavior of C-KC aerogel were investigated by simulating solid mechanics model using the finite element method. The finite element simulation is carried out by using comsol multiphysics. For investigating the deformation and elastic strength, the displacement loading is applied on the rigid plane to control the compression. Two continuous arches are used to represent a wave-shaped layer. A cubic bezeir curve is used to

describe the arches, but it adopts a straight-line shape at the contact region between arch layer and rigid plane.

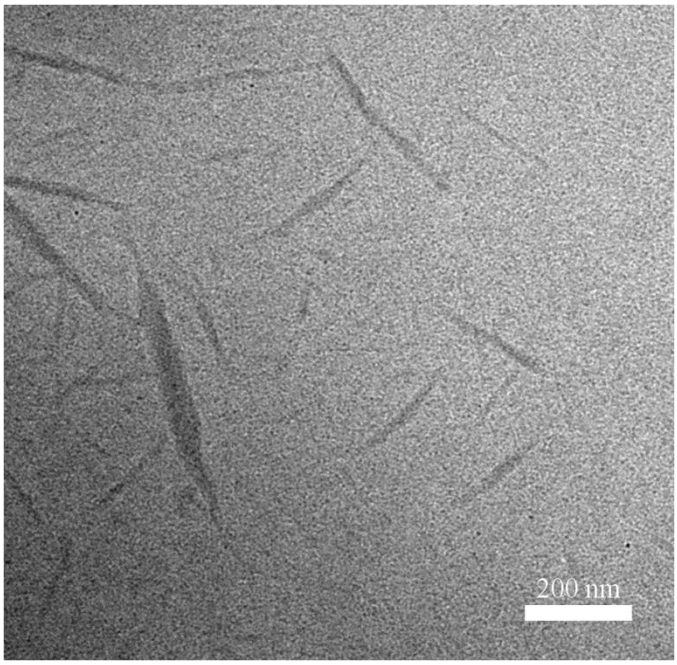

Figure S1. TEM image of CNCs.

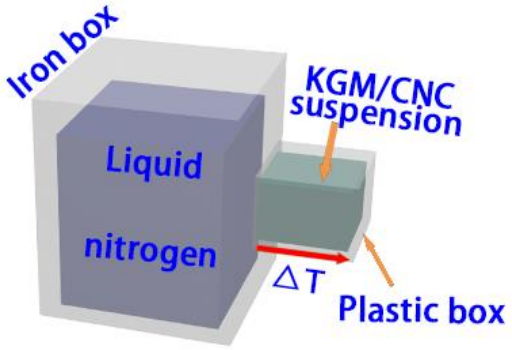

Figure S2. Schematic illustration of the freeze-casting.

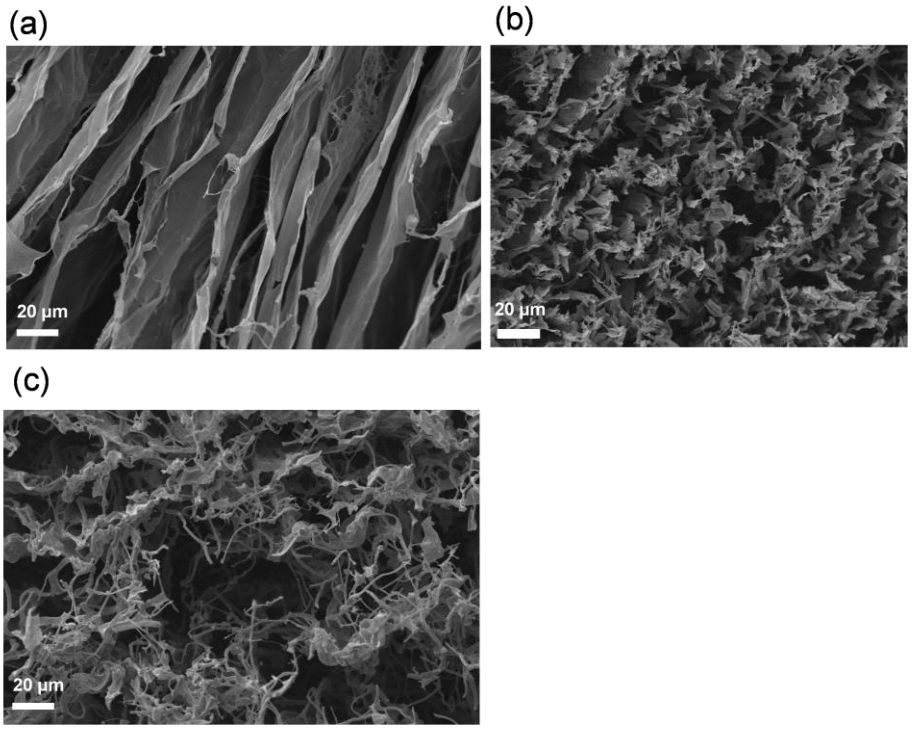

Figure S3. SEM images of KC aerogel (a), CNC aerogel (b), and KGM aerogel (c).

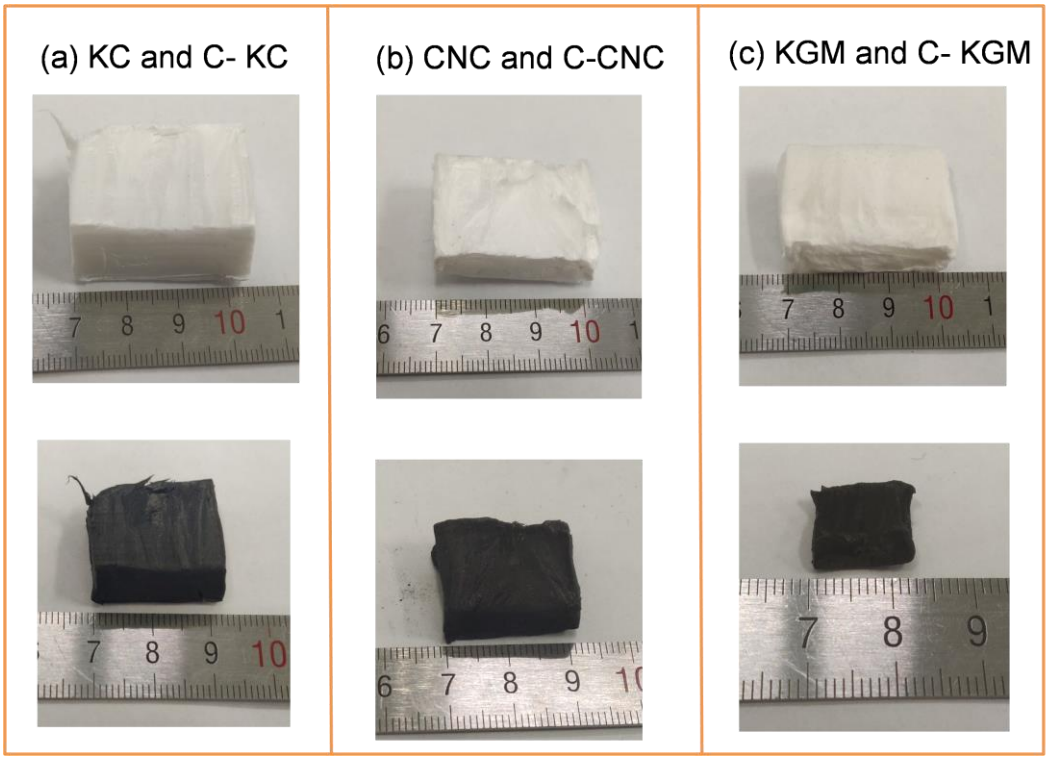

Figure S4. Digital photographs of (a) KC and C-KGM carbon aerogel, (b) CNC and C-CNC carbon aerogel, and (c) KGM and C-KGM carbon aerogel.

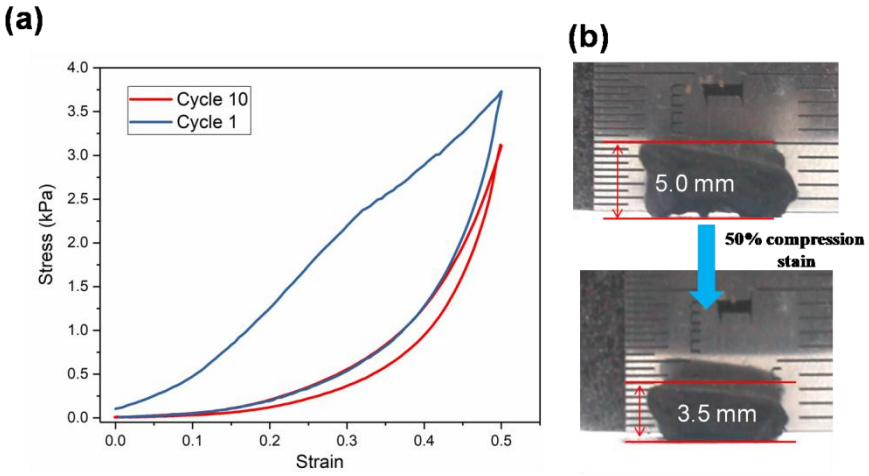

Figure S5. Stress-strain curves of C-KGM carbon aerogel at 50% compression strain for 100 cycles (a). Digital photographs of C-KGM before and after 10 cycles at a compression strain of 50% (b).

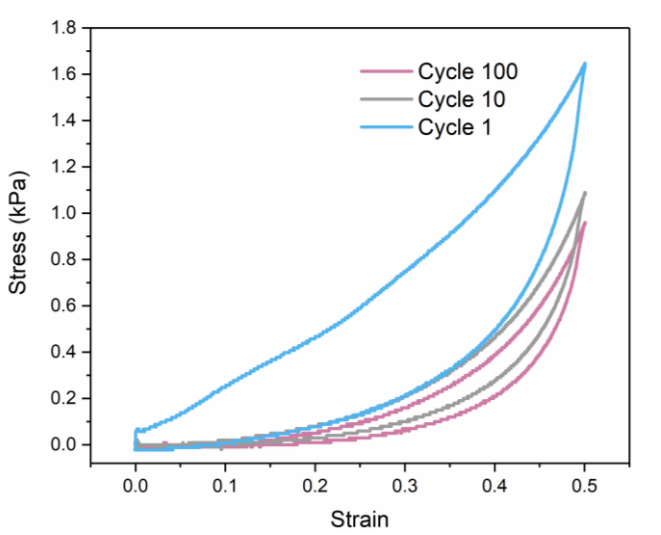

Figure S6. Stress-strain curves of C-CNC carbon aerogel at 50% compression strain for 100 cycles.

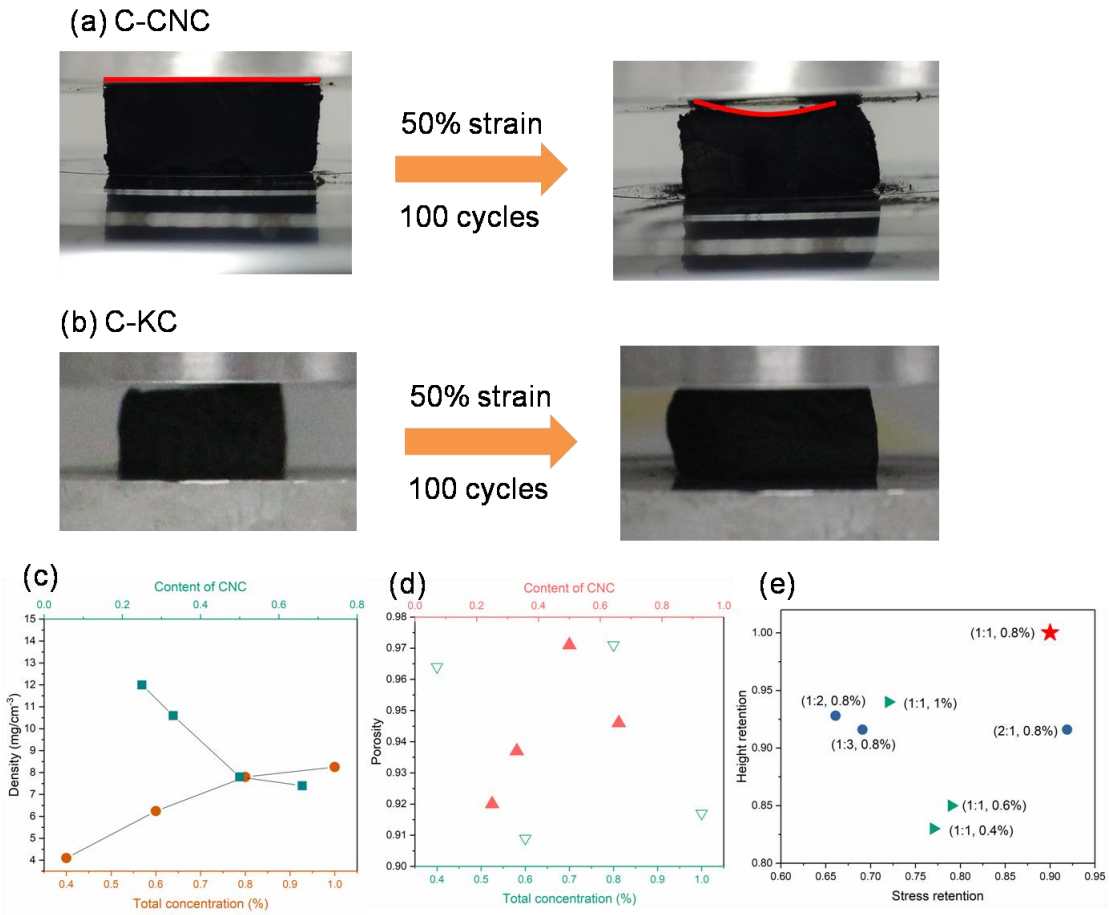

Figure S7. Digital photographs of C-CNC before and after 100 cycles at a compression strain of 50% (a). Digital photographs of C-KC before and after 100 cycles at a compression strain of 50% (b). The densities of carbon aerogels with different ratios and concentrations (c). The porosities of carbon aerogels with different ratios and concentrations (d). Mechanical performances of carbon aerogels with different ratios and concentrations (e).

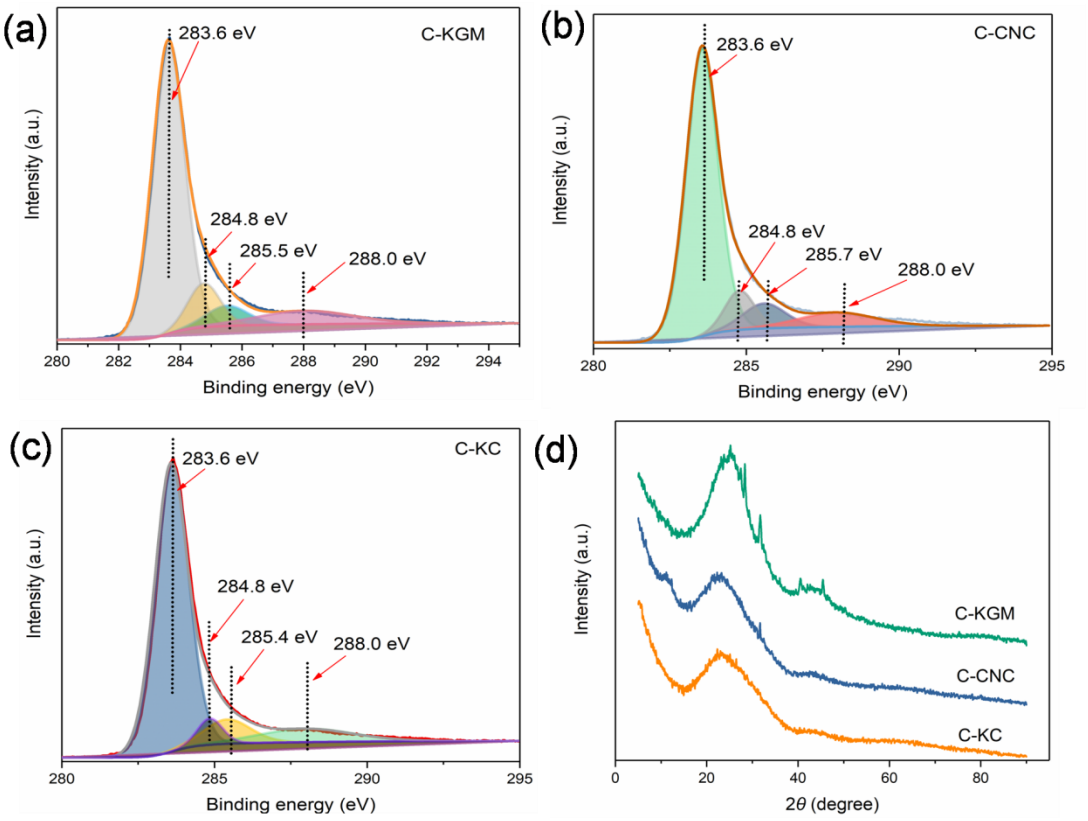

Figure S8. X-ray photoelectron spectra (XPS) of C-KGM (a), C-CNC (b), C-KC carbon aerogel (c), and XRD spectra of C-KGM, C-CNC, and C-KC (d).

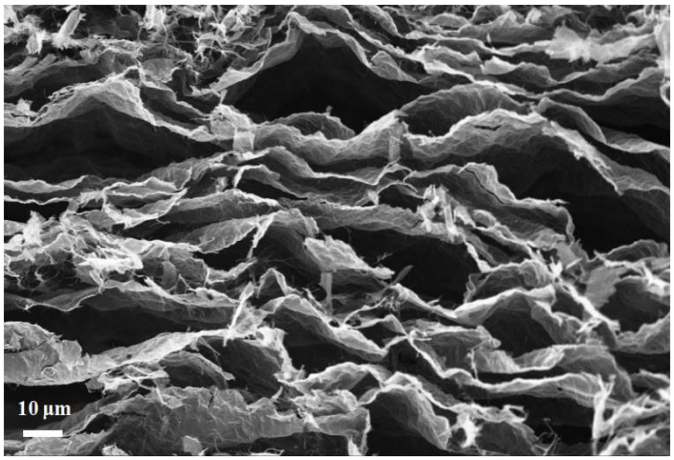

Figure S9. SEM image of C-KC after 10000 cycles at 50% strain.

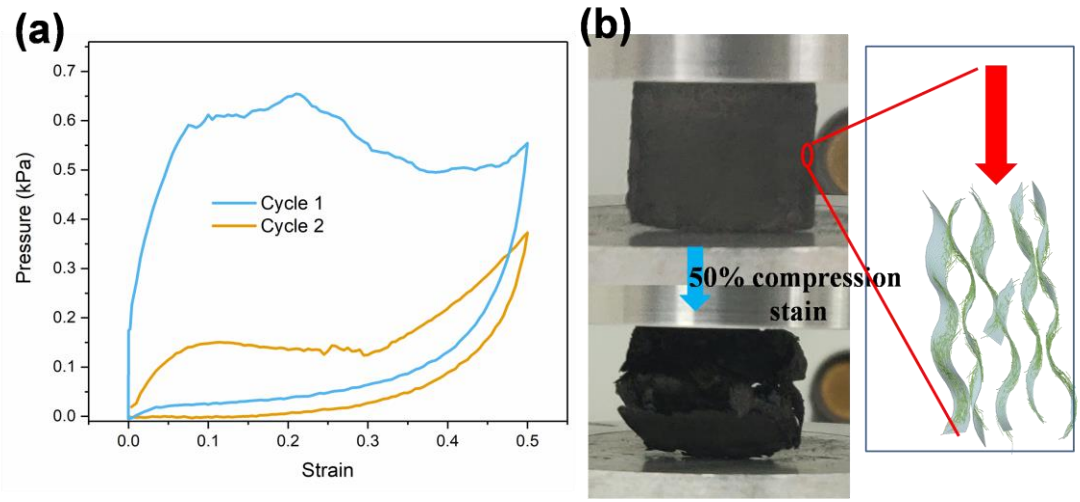

Figure S10. Stress-strain curves of C-KC at 50% compression strain for 2 cycles (along the lamella direction) (a). Digital photographs of C-KC before and after 2 cycles at a compression strain of 50% (along the lamella direction) (b).

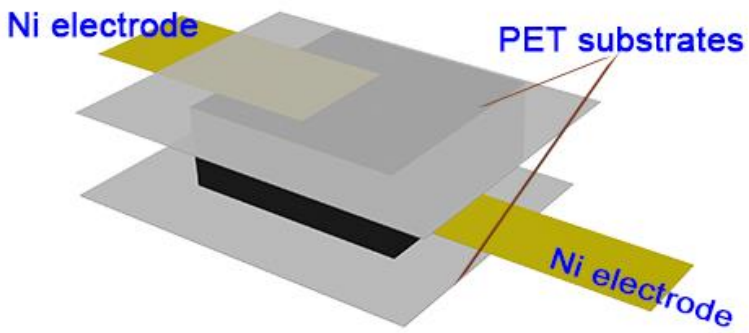

Figure S11. Schematic illustration of assembling C-KC based sensor for sensing performance testing.

Table S1. Comparison of stress and height retention of various carbon materials.

Materials	Stress retention	Height retention	Compression strain and cycle numbers	Reference
GO/CNT	88%	100%	50%, 1000	1
Carbon nanofiber aerogels	93%	98	50%, 10000	2
CNT sponge	-	80%	60%,1000	3
CNT foams	_	93	95%, 1000	4
MXene/CNC	87.9%	95.4%	50%, 10000	5
MXene/CS	68%	91.6%	50%, 10000	6
MXene/BC	73.6%	93.3%	50%, 10000	7
RF–GO	90%	88.6%	50%, 100	8
Graphene oxide aerogel	~92%	92%	50%, 15	9
C-CNC/rGO-X	71.2%	91.8%	50%, 10000	10
	55.1%	85%	99%, 100	
C–G monolith	86%	98%	50%, 250000	11
	60%	93%	80%, 10000	
UCM aerogel	72%	84.7%	60%, 1000	12

Carbonaceous nanofibrous aerogels	75%	95.7%	50%, 1000	13
Elastin hybrid cryogels	91.2%	100%	80%, 100	14
	73.2%	87.8%	97.5%, 100	
Graphene aerogel	89.8%	-	50%, 20	15
Biomimetic graphene aerogel	85%	-	50%, 1000	16
	77%		90%, 100	
C-KC carbon aerogel	90.5%	100%	50%, 10000	This work
	93%	100%	20%, 10000	
	80%	90%	90%, 1000	

Table S2. Comparison of energy loss coefficient of various aerogels.

Materials	Energy loss coefficient	Compression strain and cycle numbers	Reference
3D printed graphene aerogels	60%-30%	50%, 10	17
Macroporous graphene monoliths	65%-58%	50%, 10	18
Graphene-based aerogels	55%-44%	50%, 1000	19
Graphene elastomer	56%-45%	80%, 10	20
Wood carbon sponge	37%-25%	80%, 10	21
Graphene-based cellular monoliths	82.5%-65%	77%, 4	22
rGO-CN	86%-55%	50%,4	23
Holey graphene aerogel	48.8%-35.76%	50%, 20	24
Carbonaceous nanofibrous aerogels	42%-32%	50%, 1000	25
GO/CS	36%-26%	80%, 10	11
CNT composite	64%-42%	70%, 100	26
CNT array(sponge)	80%	80%, 1	27
C-KC carbon aerogel	18.6%	20%, 10000	This wok

	28.3%	50%, 10000
	37.7%	90%, 1000

Table S3. Comparison of sensitivity of various aerogels.

Materials	Sensitivity (kPa^{-1})	Reference
Carbonaceous nanofibrous aerogels	1.02	25
CuNWs	0.7	28
rGO/PI	0.18	29
Graphene aerogels	0.18	30
Graphene–Polyurethane Sponge	0.26	31
CB@PU	0.068	32
Hard Carbon Nanofiber Aerogels	0.057	2
C-KC carbon aerogel	6.83	This work

Movie S1. The comparison of C-KC at a strain of 95%.

Movie S2. The comparison of C-KC at a strain of 50%.

Movie S3. Simulated compression process of C-KC from finite element method.

References

(1) Haiyan, S.; Zhen, X.; Chao, G., Multifunctional, ultra-flyweight, synergistically assembled carbon aerogels. *Adv. Mater.* **2013,** *25*, 2554-2560.

(2) Yu, Z.-L.; Qin, B.; Ma, Z.-Y.; Huang, J.; Li, S.-C.; Zhao, H.-Y.; Li, H.; Zhu, Y.-B.; Wu, H.-A.; Yu, S.-H., Superelastic Hard Carbon Nanofiber Aerogels. *Adv. Mater.* **2019,** *31*, 1900651.

(3) Gui, X. C.; Wei, J. Q.; Wang, K. L.; Cao, A. Y.; Zhu, H. W.; Jia, Y.; Shu, Q. K.; Wu, D. H., Carbon nanotube sponges. *Adv. Mater.* **2010,** *22*, 617-621.

(4) Wang, H.; Lu, W.; Di, J.; Li, D.; Zhang, X.; Li, M.; Zhang, Z.; Zheng, L.; Li, Q., Ultra-Lightweight and Highly Adaptive All-Carbon Elastic Conductors with Stable Electrical Resistance. *Adv. Funct. Mater.* **2017,** *27*, 1606220.

(5) Zhuo, H.; Hu, Y.; Chen, Z.; Peng, X.; Liu, L.; Luo, Q.; Yi, J.; Liu, C.; Zhong, L., A carbon aerogel with super mechanical and sensing performances for wearable piezoresistive sensors. *J. Mater. Chem. A* **2019, 7**, 8092-8100.

(6) Hu, Y.; Zhuo, H.; Luo, Q.; Wu, Y.; Sun, R., Biomass polymer-assisted fabrication of aerogels from MXenes with ultrahigh compression elasticity and pressure sensitivity. *J. Mater. Chem. A* **2019,** 7, 10273-10281.

(7) Chen, Z.; Hu, Y.; Zhuo, H.; Liu, L.; Jing, S.; Zhong, L.; Peng, X.; Sun, R.-c., Compressible, elastic, and pressure-sensitive carbon aerogel derived from 2D titanium carbide nanosheets and bacterial cellulose for wearable sensors. *Chem. Mater.* **2019,** 31,3301-3312.

(8) Wang, X.; Lu, L. L.; Yu, Z. L.; Xu, X. W.; Zheng, Y. R.; Yu, S. H., Scalable Template Synthesis of Resorcinol-Formaldehyde/Graphene Oxide Composite Aerogels with Tunable Densities and Mechanical Properties. *Angew. Chem. Int. Edit.* **2015,** *54*, 2397-401.

(9) Wang, C.; Chen, X.; Wang, B.; Huang, M.; Wang, B.; Jiang, Y.; Ruoff, R. S., Freeze-Casting Produces a Graphene Oxide Aerogel with a Radial and Centrosymmetric Structure. *ACS Nano* **2018,** 12, 65816-5825.

(10) Zhuo, H.; Hu, Y.; Tong, X.; Chen, Z.; Zhong, L.; Lai, H.; Liu, L.; Jing, S.; Liu, Q.; Liu, C., A Supercompressible, Elastic, and Bendable Carbon Aerogel with Ultrasensitive Detection Limits for Compression Strain, Pressure, and Bending Angle. *Adv. Mater.* **2018**, 30, 1706705.

(11) Gao, H. L.; Zhu, Y. B.; Mao, L. B.; Wang, F. C.; Luo, X. S.; Liu, Y. Y.; Lu, Y.; Pan, Z.; Ge, J.; Shen, W., Super-elastic and fatigue resistant carbon material with lamellar multi-arch microstructure. *Nat. Commun.* **2016,** *7*, 12920-12929.

(12) Zhang, J.; Li, B.; Li, L.; Wang, A., Ultralight, compressible and multifunctional carbon aerogels based on natural tubular cellulose. *J. Mater. Chem. A* **2016,** *4*, 2069-2074.

(13) Si, Y.; Wang, X.; Yan, C.; Yang, L.; Yu, J.; Ding, B., Ultralight Biomassâ□□Derived Carbonaceous Nanofibrous Aerogels with Superelasticity and High Pressureâ□□Sensitivity. *Adv. Mater.* **2016,** *28*, 9512-9518.

(14) Liu, Y.; Xu, K.; Chang, Q.; Darabi, M. A.; Lin, B.; Zhong, W.; Xing, M., Highly Flexible and Resilient Elastin Hybrid Cryogels with Shape Memory, Injectability, Conductivity, and Magnetic Responsive Properties. *Adv. Mater.* **2016,** *28*, 7758-7767.

(15) Kotal, M.; Kim, H.; Roy, S.; Oh, I. K., Sulfur and nitrogen co-doped holey graphene aerogel for structurally resilient solid-state supercapacitors under high compressions. *J. Mater. Chem. A* **2017,** *5*, 17253-17266.

(16) Yang, M.; Zhao, N.; Cui, Y.; Gao, W.; Zhao, Q.; Gao, C.; Bai, H.; Xie, T., Biomimetic Architectured Graphene Aerogel with Exceptional Strength and Resilience. *ACS Nano* **2017,** *11*

6817-6824.

(17) Zhu, C.; Han, T. Y.; Duoss, E. B.; Golobic, A. M.; Kuntz, J. D.; Spadaccini, C. M.; Worsley, M. A., Highly compressible 3D periodic graphene aerogel microlattices. *Nat. Commun.* **2015,** *6*, 6962-6969.

(18) Yingru, L.; Ji, C.; Liang, H.; Chun, L.; Jong-Dal, H.; Gaoquan, S., Highly compressible macroporous graphene monoliths via an improved hydrothermal process. *Adv. Mater.* **2014,** *26*, 4789-4793.

(19) Ji, L.; Liu, Y.; Zhang, H. B.; Yang, D.; Liu, Z.; Yu, Z. Z., Superelastic and multifunctional graphene based aerogels by interfacial reinforcement with graphitized carbon at high temperatures. *Carbon* **2018,** *132*, 95-103.

(20) Qiu, L.; Huang, B.; He, Z.; Wang, Y.; Tian, Z.; Liu, J. Z.; Wang, K.; Song, J.; Gengenbach, T. R.; Li, D., Extremely Low Density and Super-Compressible Graphene Cellular Materials. *Adv. Mater.* **2017,** *29*, 1701553.

(21) Chen, C.; Song, J.; Zhu, S.; Li, Y.; Kuang, Y.; Wan, J.; Kirsch, D.; Xu, L.; Wang, Y.; Gao, T., Scalable and Sustainable Approach toward Highly Compressible, Anisotropic, Lamellar Carbon Sponge. *Chem* **2018,** *4*, 1-11.

(22) Ling, Q.; Liu, J. Z.; Chang, S. L. Y.; Wu, Y.; Dan, L., Biomimetic superelastic graphene-based cellular monoliths. *Nat. Commun.* **2012,** *3*, 1241-1247.

(23) Barg, S.; Perez, F. M.; Ni, N.; Do, V. P. P.; Maher, R. C.; Garcia-Tuã±On, E.; Eslava, S.; Agnoli, S.; Mattevi, C.; Saiz, E., Mesoscale assembly of chemically modified graphene into complex cellular networks. *Nat. Commun.* **2014,** *5*, 4328-4337.

(24) Kotal, M.; Kim, H.; Roy, S.; Oh, I., Sulfur and Nitrogen Co-Doped Holey Graphene Aerogel for

Structurally Resilient Solid-State Supercapacitors under High-Compressions. *J. Mater. Chem. A 5*, 17253-17266.

(25) Si, Y.; Wang, X.; Yan, C.; Yang, L.; Yu, J.; Ding, B., Ultralight Biomass-Derived Carbonaceous Nanofibrous Aerogels with Superelasticity and High Pressure-Sensitivity. *Adv. Mater.* **2016,** *28*, 9655-9655.

(26) Zhiping, Z.; Xuchun, G.; Qiming, G.; Zhiqiang, L.; Yuan, Z.; Wenhui, Z.; Rong, X.; Anyuan, C.; Zikang, T., Integrated random-aligned carbon nanotube layers: deformation mechanism under compression. *Nanoscale* **2014,** *6* (3), 1748-1755.

(27) Xuchun, G.; Zhiping, Z.; Yuan, Z.; Hongbian, L.; Zhiqiang, L.; Qiming, G.; Rong, X.; Anyuan, C.; Zikang, T., Three-dimensional carbon nanotube sponge-array architectures with high energy dissipation. *Adv. Mater.* **2014,** *26* (8), 1248-1253.

(28) Xu, X.; Wang, R.; Nie, P.; Cheng, Y.; Lu, X.; Shi, L.; Sun, J., Copper Nanowire-Based Aerogel with Tunable Pore Structure and Its Application as Flexible Pressure Sensor. *Acs Appl. Mater. Interfaces* **2017,** *9*, 14273-14280.

(29) Yuyang, Q.; Qingyu, P.; Yujie, D.; Zaishan, L.; Chunhui, W.; Ying, L.; Fan, X.; Jianjun, L.; Ye, Y.; Xiaodong, H., Lightweight, Superelastic, and Mechanically Flexible Graphene/Polyimide Nanocomposite Foam for Strain Sensor Application. *ACS Nano* **2015,** *9*, 8933-8941.

(30) Li, C.; Jiang, D.; Hui, L.; Huo, B.; Liu, C.; Yang, W.; Liu, J., Superelastic and Arbitrary-Shaped Graphene Aerogels with Sacrificial Skeleton of Melamine Foam for Varied Applications. *Adv. Funct. Mater.* **2017,** *28*, 1704674.

(31) Hong-Bin, Y.; Jin, G.; Chang-Feng, W.; Xu, W.; Wei, H.; Zhi-Jun, Z.; Yong, N.; Shu-Hong, Y., Pressure sensors: a flexible and highly pressure-sensitive graphene-polyurethane sponge based on

fractured microstructure design (adv. Mater. 46/2013). *Adv. Mater.* **2013,** *25*, 6691-6691.

(32) Wu, X.; Han, Y.; Zhang, X.; Zhou, Z.; Lu, C., Large-Area Compliant, Low-Cost, and Versatile Pressure-Sensing Platform Based on Microcrack-Designed Carbon Black@Polyurethane Sponge for Human-Machine Interfacing. *Adv. Funct. Mater.* **2016,** *26*, 6246-6256.